

Supplementary Figures

Fig.S1: Processing of transcriptomic, proteomic and acetylomic sequencing data.

Principal component analysis for transcriptomics (a), proteomics (b), and acetylomics (c) sequencing data.

Fig.S2: Volcano plots for DEGs and DEPs.

(a) Volcano plot of DEGs between BLCA and controls in transcriptomic sequencing dataset. (b) Volcano plot of DEPs between BLCA and controls in proteomics dataset.

Fig.S3: GO and KEGG enrichment analysis of DEGs, DEPs and DEPAs.

GO enrichment analysis showing the biological processes (BP), cellular component (CC), and molecular function (MF) enriched by DEGs (a), DEPs (c), DEPAs (e). KEGG enrichment analysis displaying pathways involved in DEGs (b), DEPs (d), DEPAs (f).

Fig.S4: Intersection of DEGs and DEPs with the same expression trends.

(a) Intersection of up-regulated DEGs and DEPs to obtain up-regulated intersecting genes. (b) Venn diagram of down-regulated DEGs and DEPs to acquire down-regulated intersecting genes.

Fig.S5: RNA-Seq data quality control and sample characterisation.

(a, b) The number of nFeature RNA and nCount RNA after quality control. (c) Principal component analysis for the samples. (d) Elbowplot for identifying the optimal principal components. The proportion of 5 cell types in samples (e), as well as BLCA tumor tissue and control groups (f).

Fig.S6: Screening of intercellular hypervariable genes.

Fig.S7: Circle plot of correlations between key genes.

Fig.S8: Heatmap of cell cluster ratios of fibroblasts and myeloid macrophages in BLCA tumour tissue versus controls.

Heat maps revealing the proportion of 7 cell clusters formed by fibroblasts (a) and myeloid macrophages (b). The proportion of 7 cell clusters formed by fibroblasts (c) and myeloid macrophages (d) in BLCA tumor tissue and control groups respectively.

Fig.S9: Expression of key genes in different branches of fibroblasts and myeloid macrophages and number of ligand-receptor pairs for cell-cell interactions.

Expression of pivotal genes in different branches of fibroblasts (a) and myeloid macrophages (b). (c) The number of ligand-receptor pairs for cell-cell interactions.

Fig.S10: Analysis of differentially expressed genes associated with BLCA between the two clusters.

Volcano plot (a) and heat map (b) of Cluster-DEGs between 2 clusters. Identification of GO (c) and KEGG (d) entries involved by Cluster-DEGs. Volcano plot (e) and heat map (f) of BLCA-DEGs between BLCA and controls in TCGA-BLCA dataset.

Fig.S11: PH assumptions for verifying the applicability of the univariate Cox regression model.

Fig.S12: Validation of risk models in GSE13507 dataset.

Risk curve (a) and K-M curve (b) predicting the overall survival and survival probability of high- and low-risk patients in GSE13507 dataset. (c) ROC curves to evaluate the predictive performance of risk model in GSE13507 dataset.

Fig.S13: The sankey plot showing the flow between different clinicopathological features.

Fig.S14: K-M survival stratification analyses.

The differences in survival probability of age ≤ 60 years (a), age > 60 years (b); pathological T1 + T2 (c), pathological T3 + T4 (d); pathological N0 (e); pathological N1 (f).

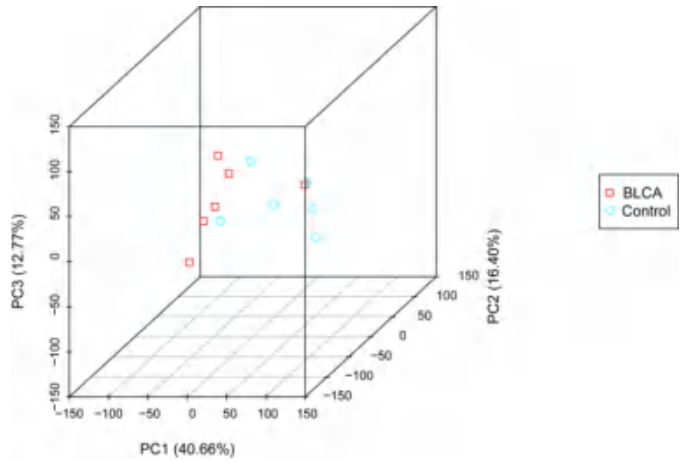
Fig.S15: Comparison of TMB differences and mutation rates of TP53 and KDM6A genes between high and low risk groups.

(a) The TMB differences between high- and low-risk teams. The mutation rate of TP53 (b) and KDM6A (c) between high- and low-risk teams.

Fig.S16: Lollipop plots depicting immune cell relationships with CASQ2, CTSE, FXYD6, MAP1A, and XAGE2.

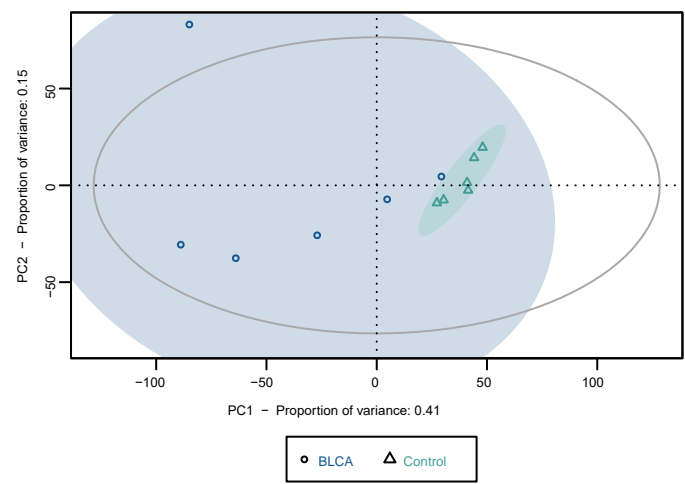
Lollipop plots illustrating the relationships between discrepant immune cells and CASQ2 (a), CTSE (b), FXYD6 (c), MAP1A (d) and XAGE2 (e).

a



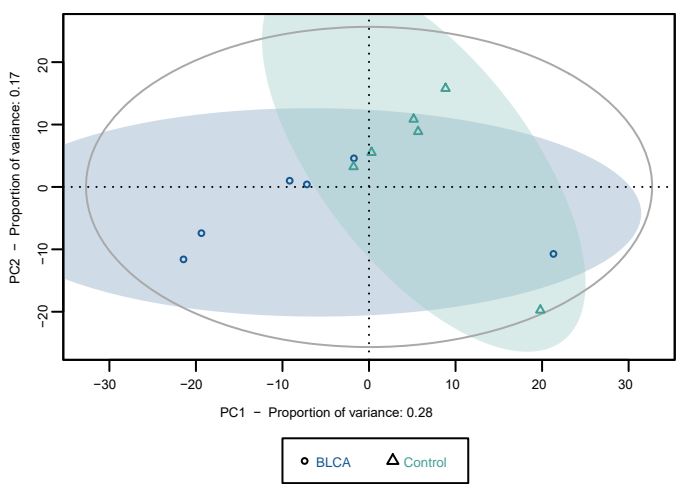
b

Principal Component Analysis

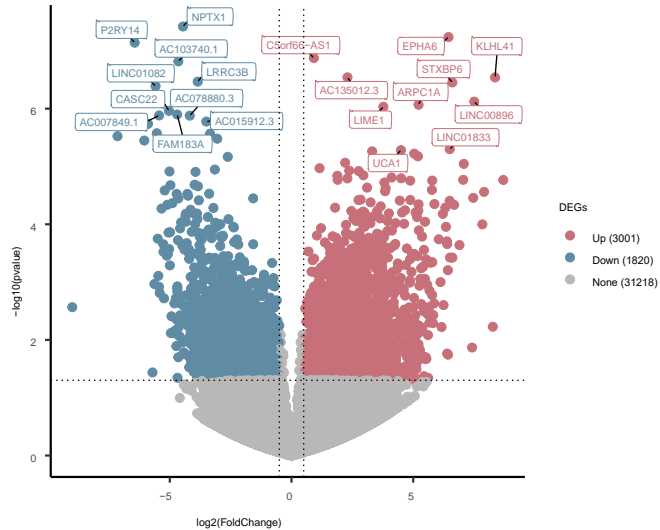


c

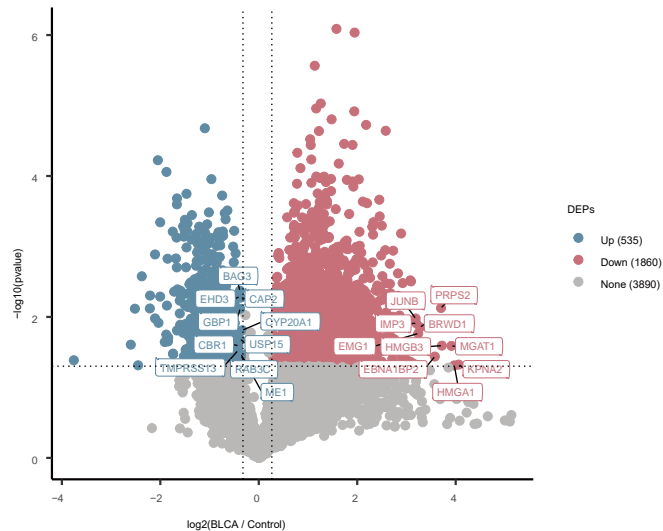
Principal Component Analysis



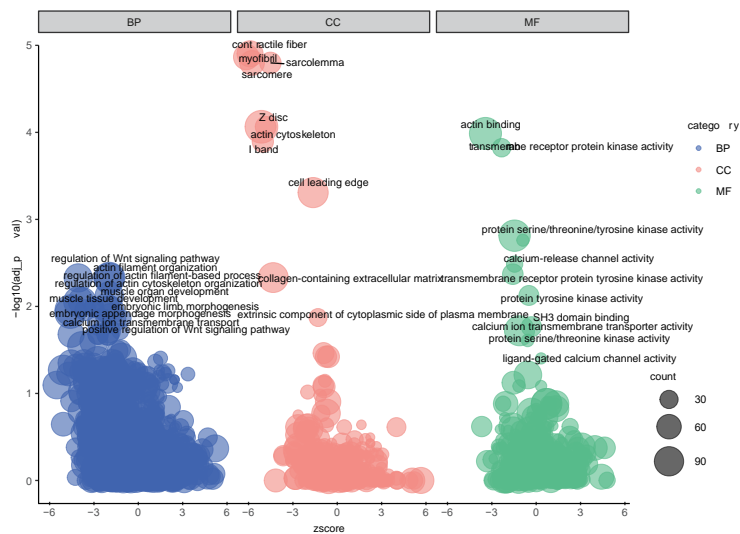
a



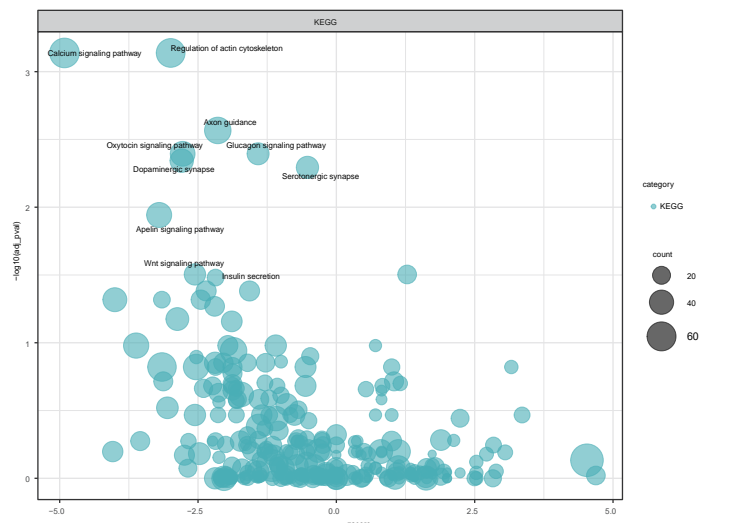
b



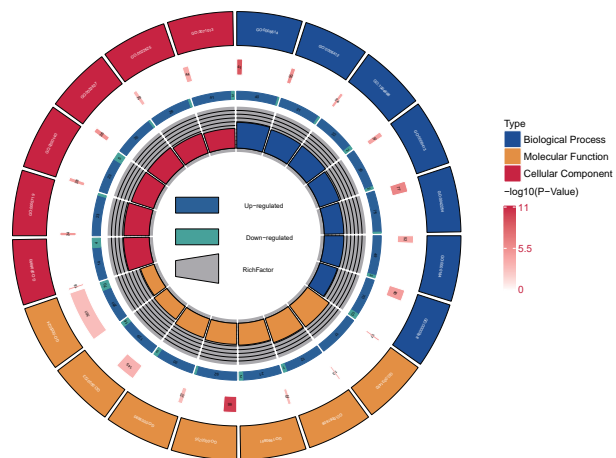
a



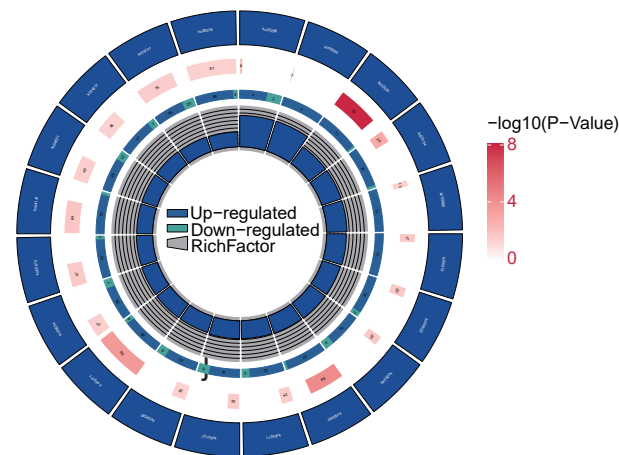
b



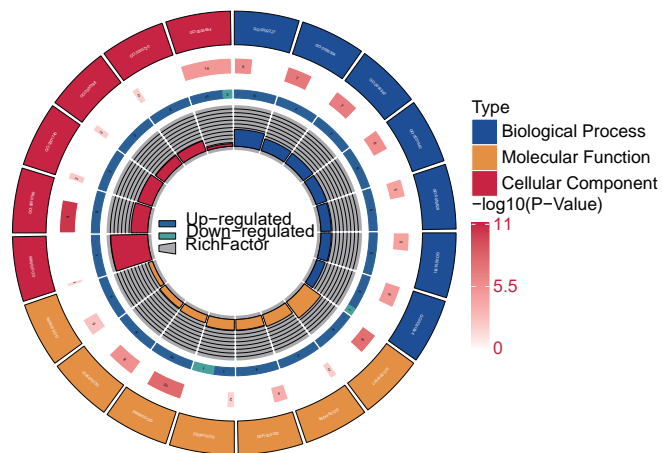
c



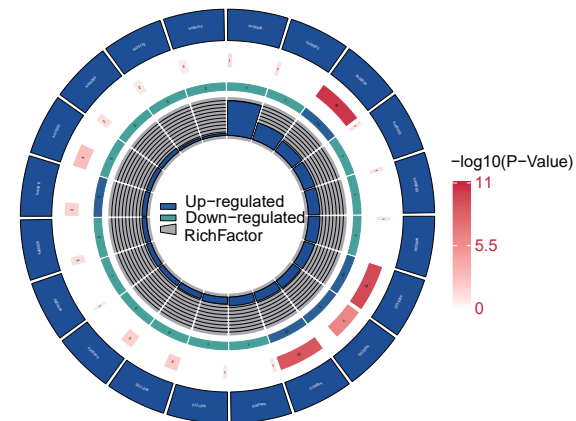
d

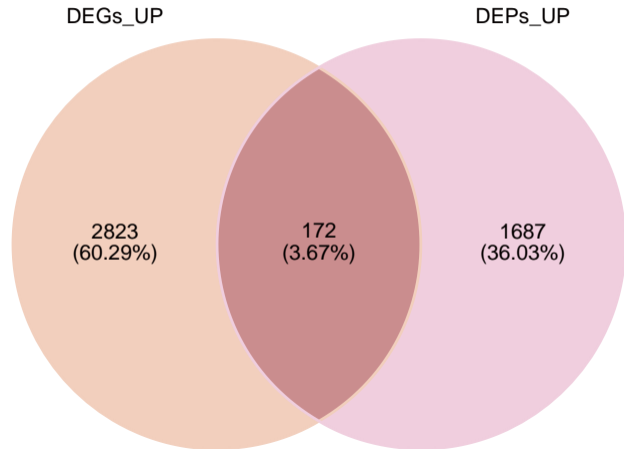
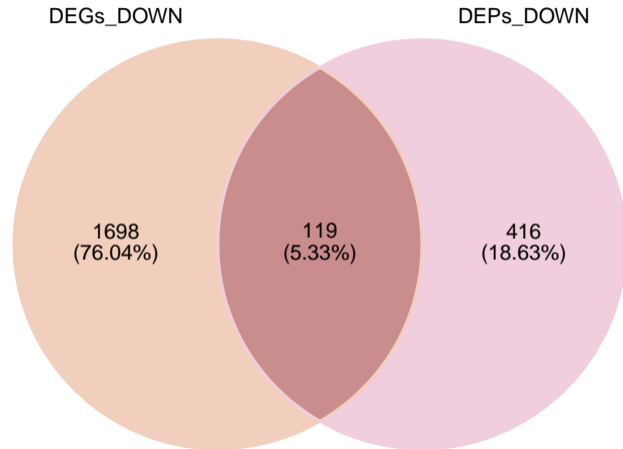


e

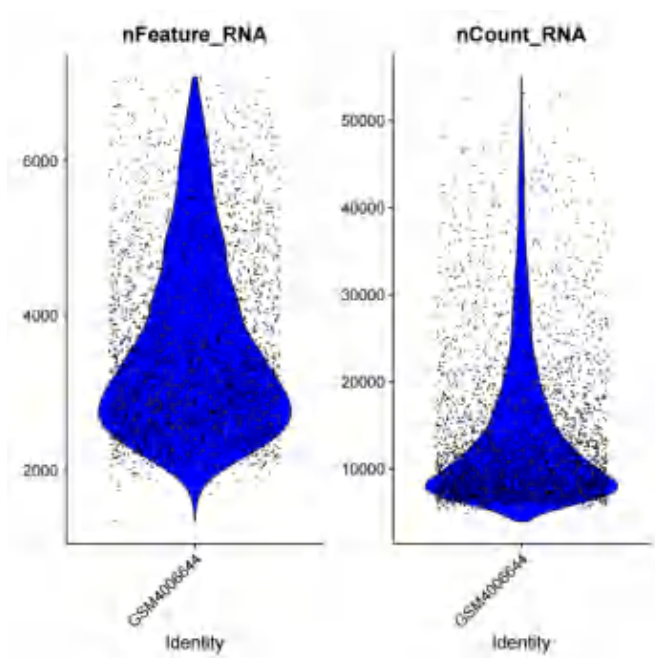


f

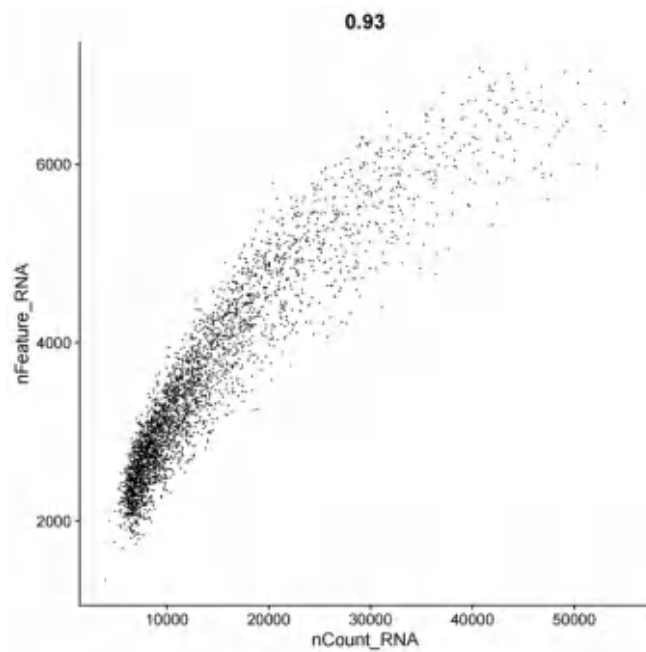


a**b**

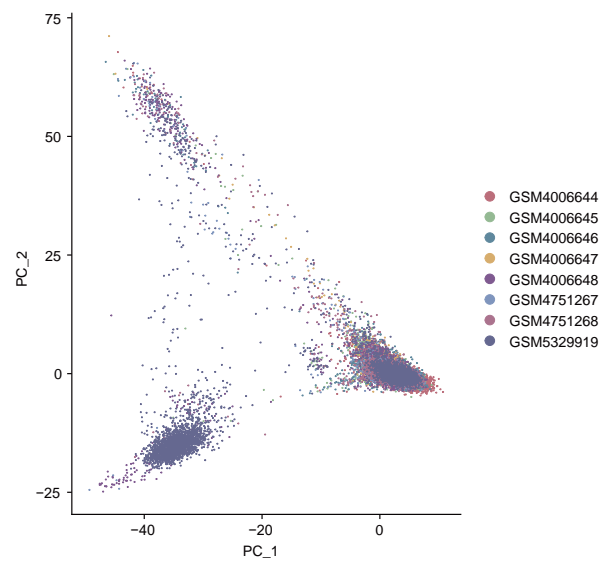
a



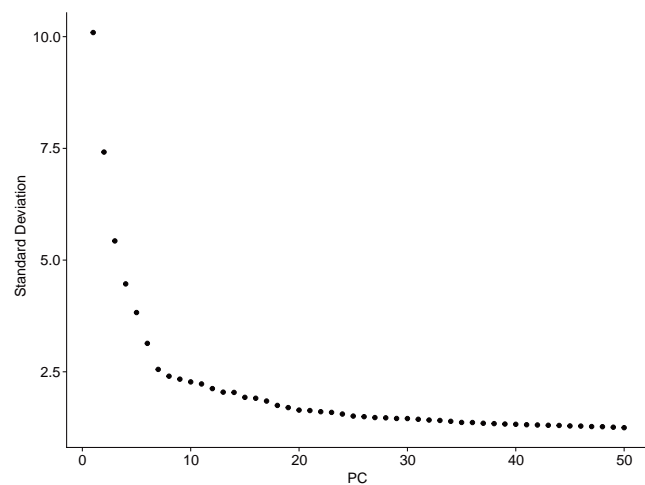
b



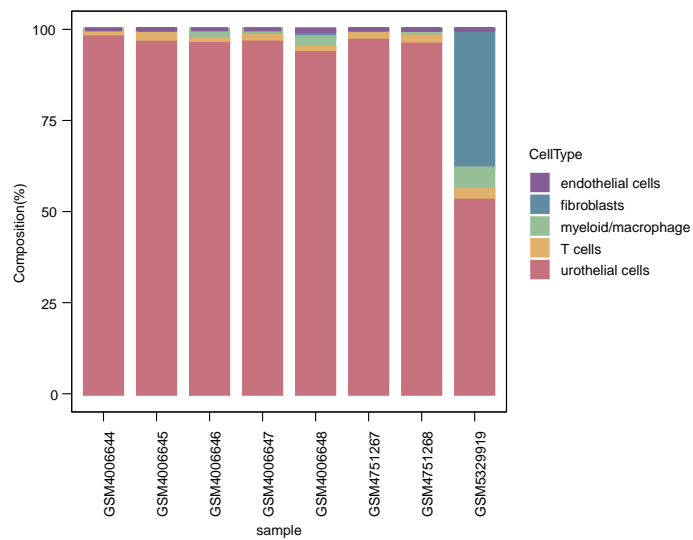
c



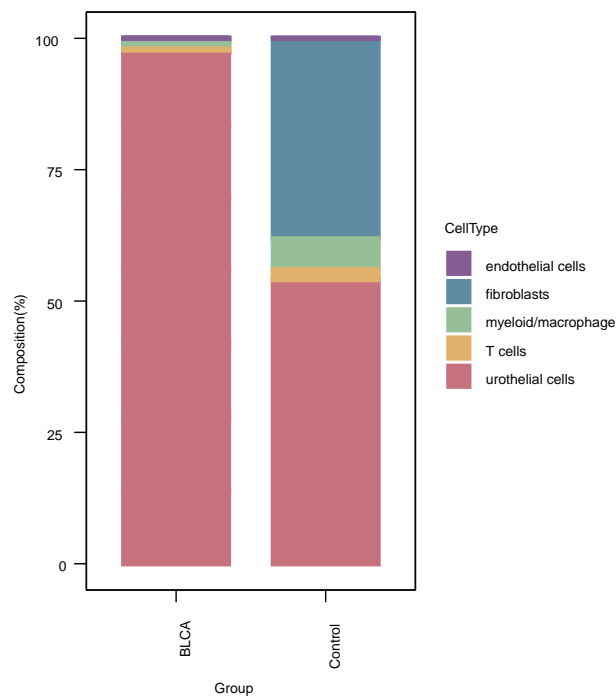
d

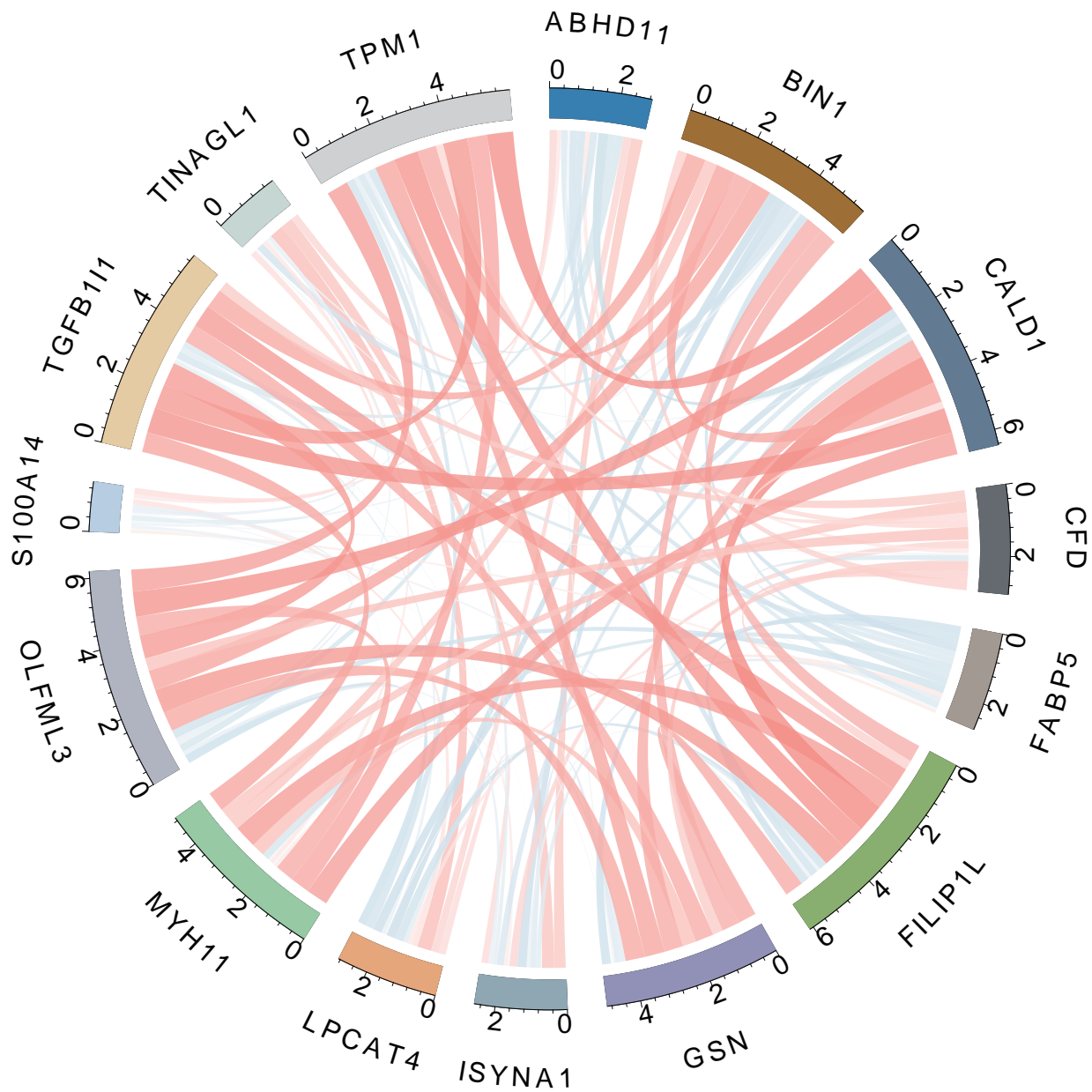


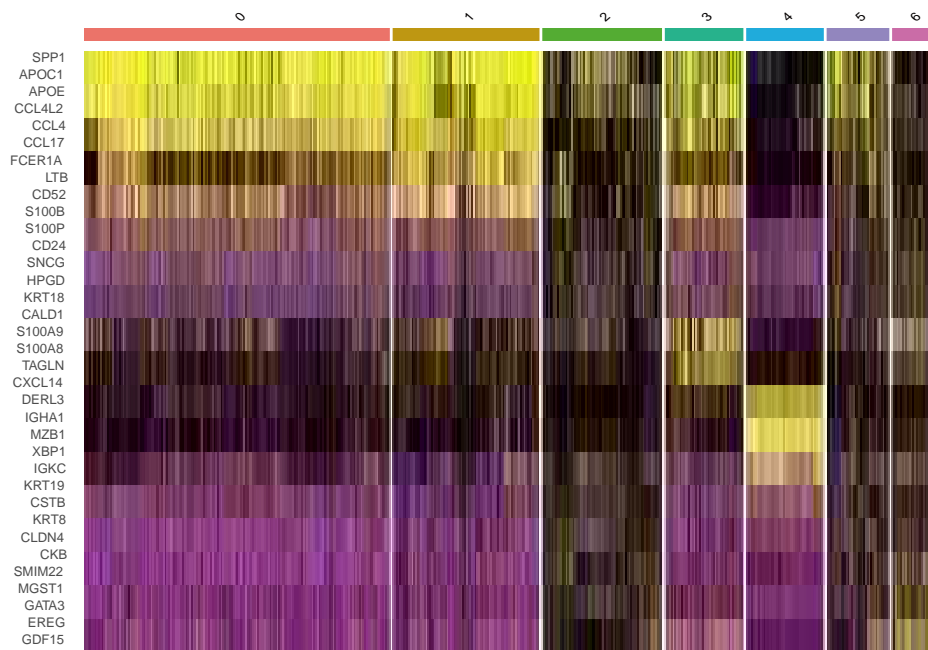
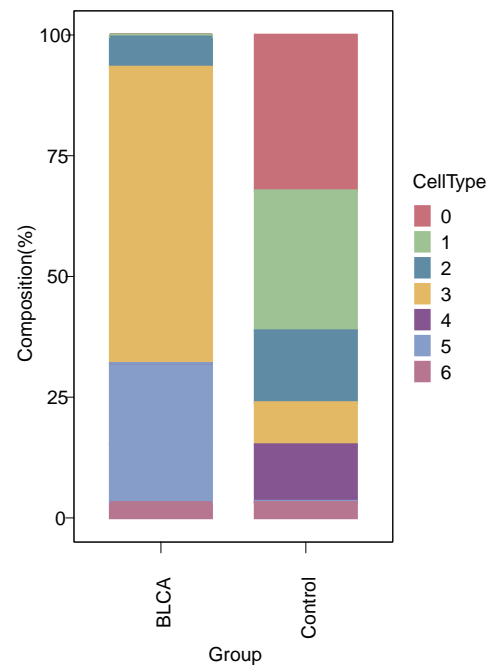
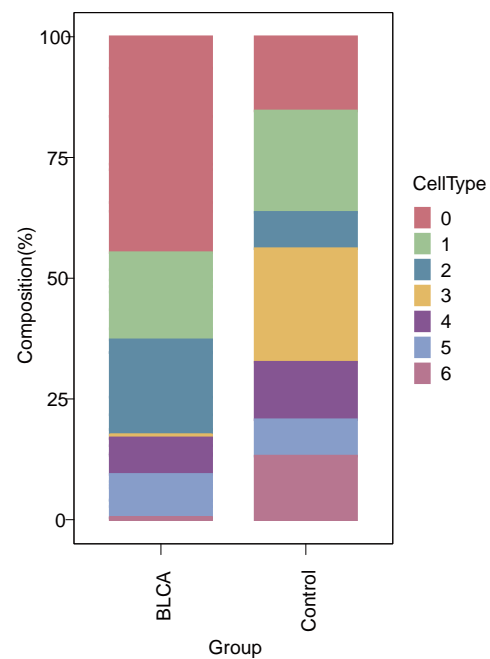
e

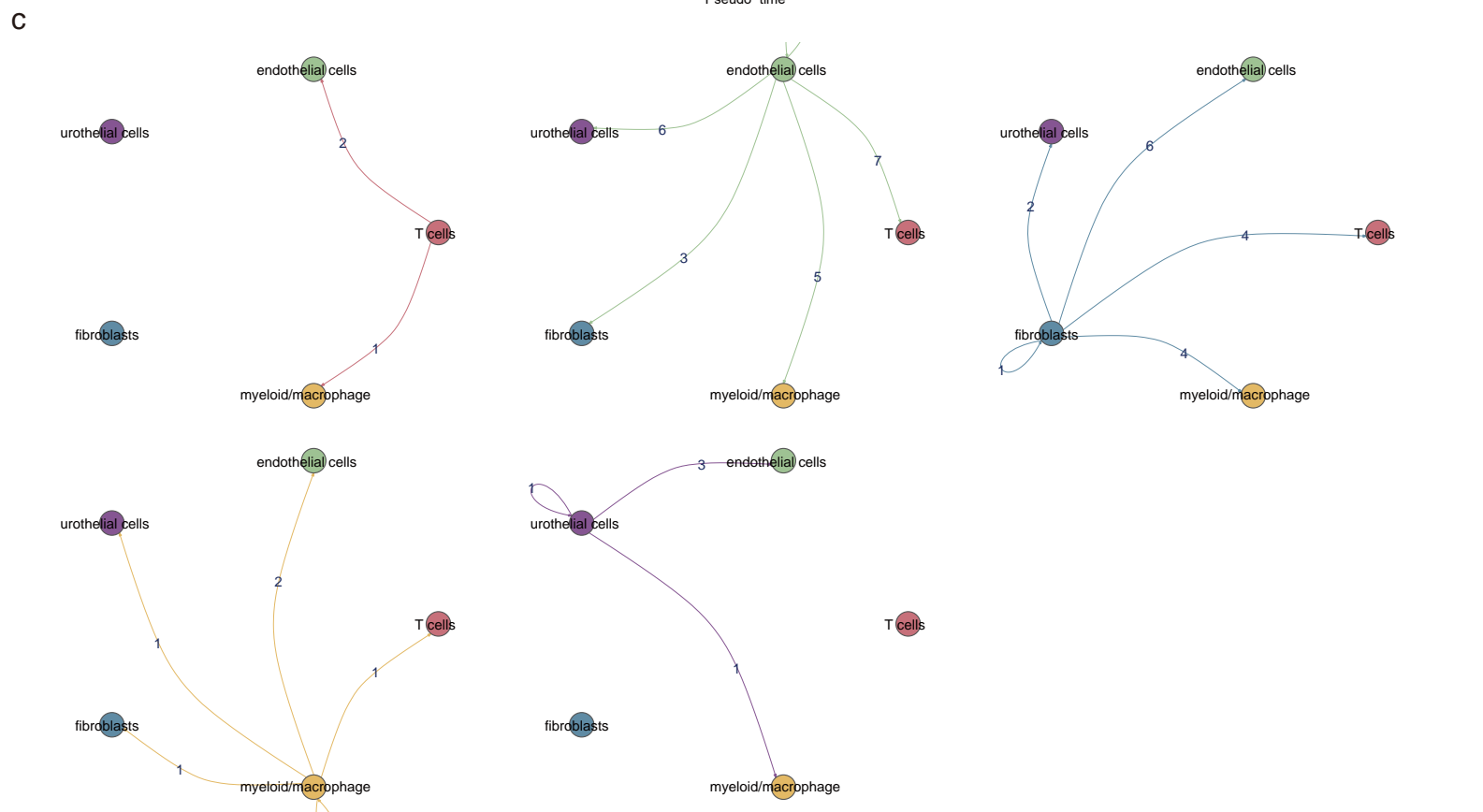
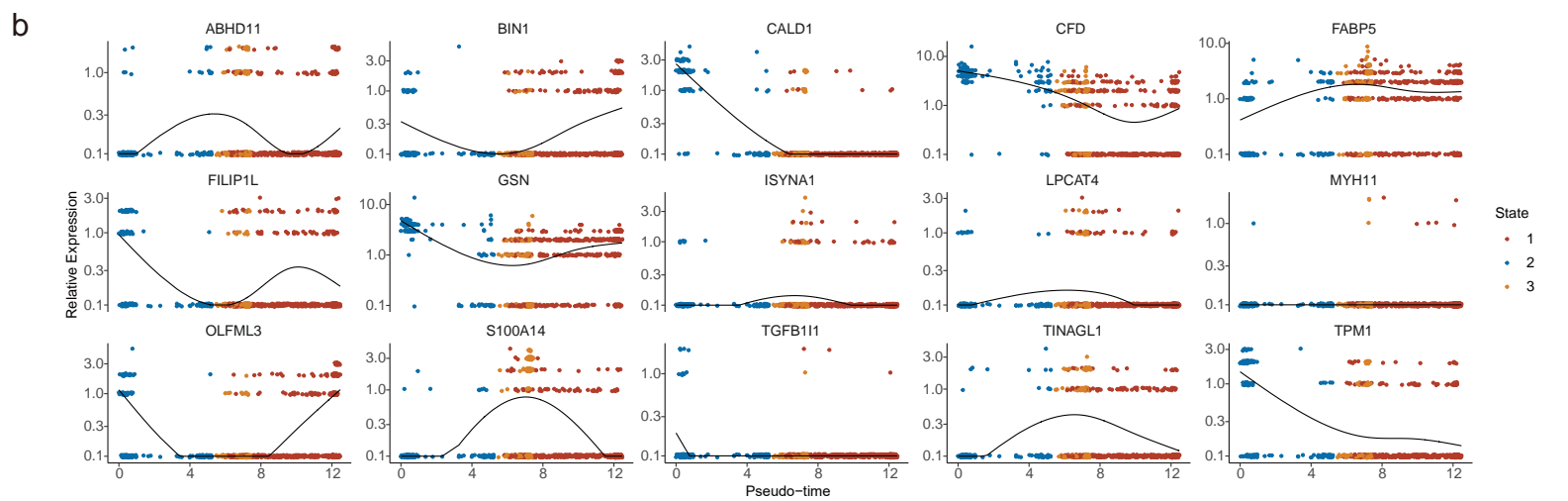
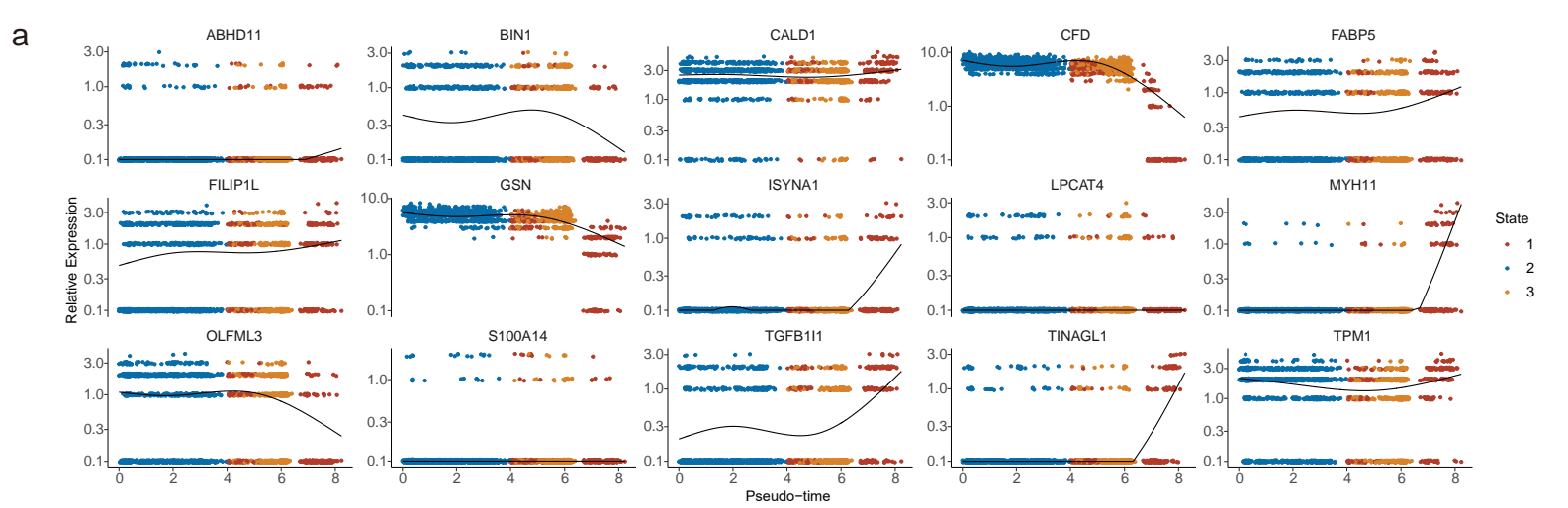


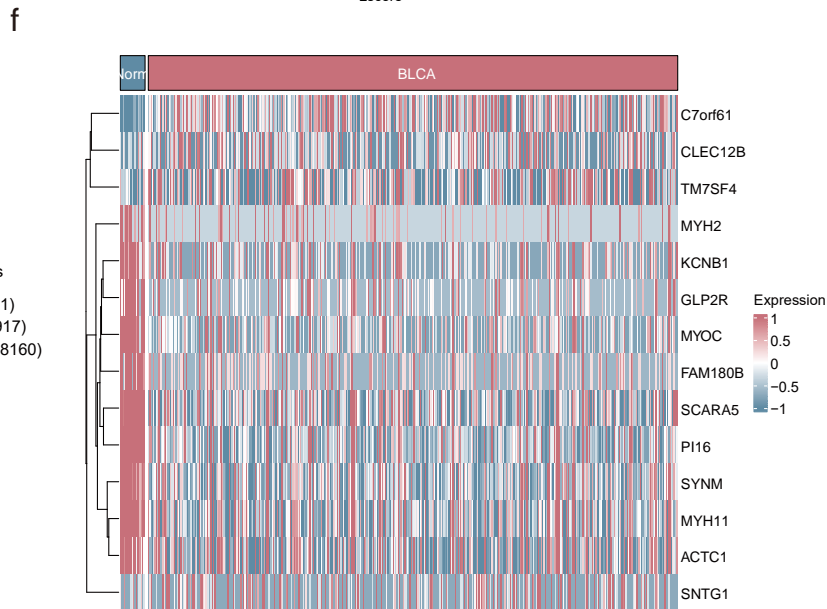
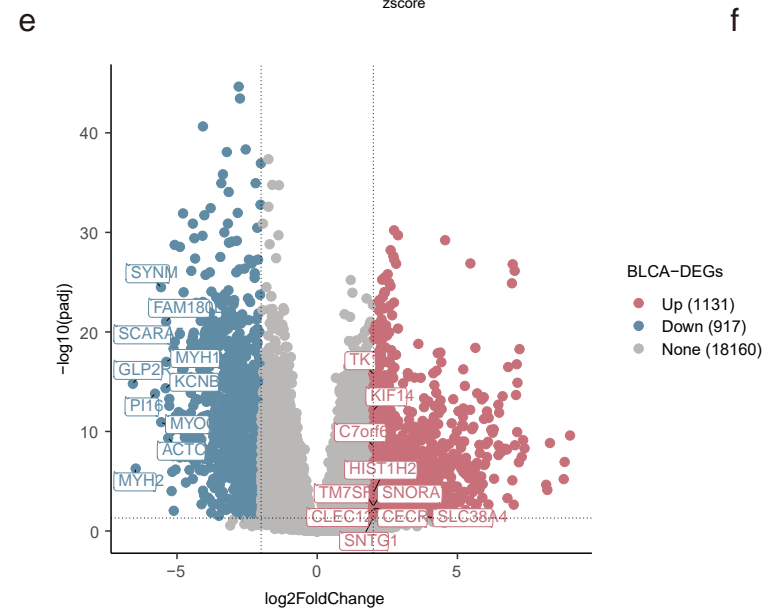
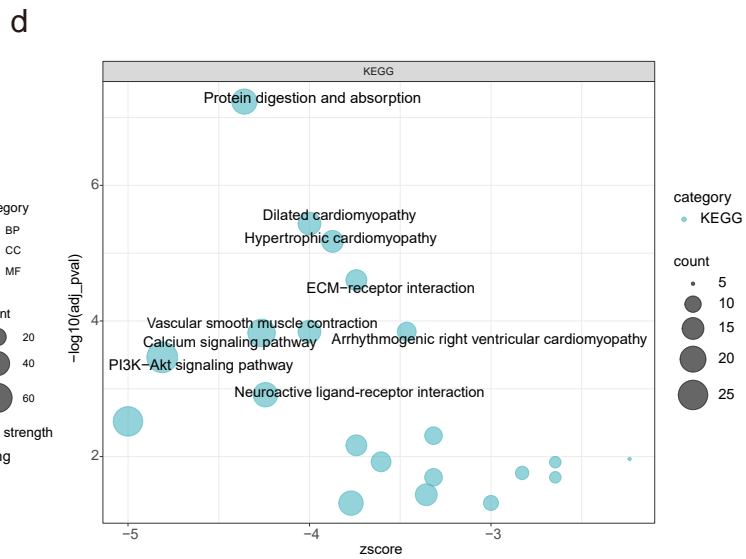
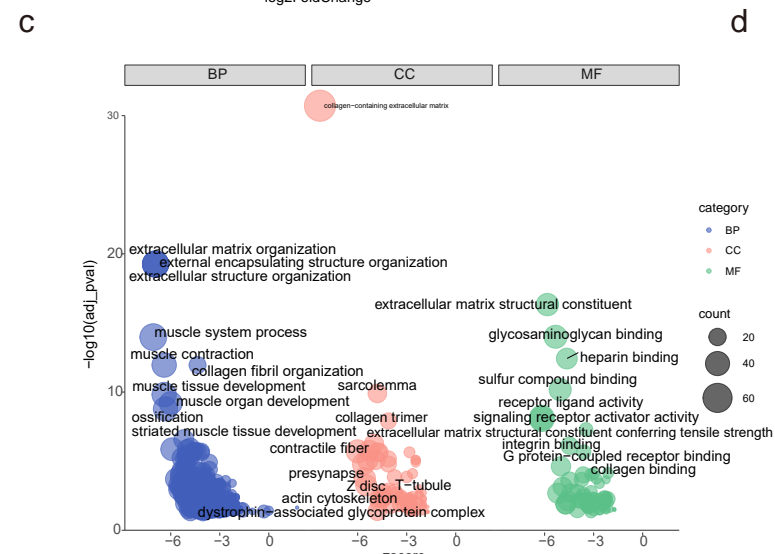
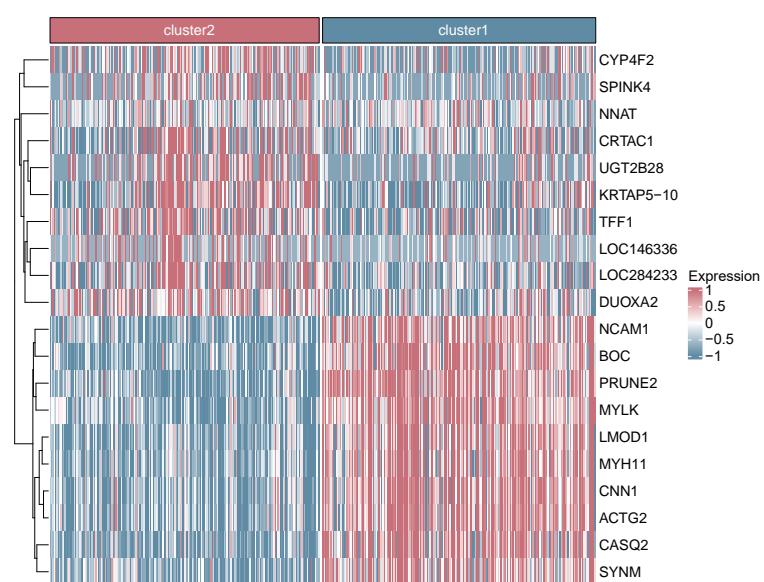
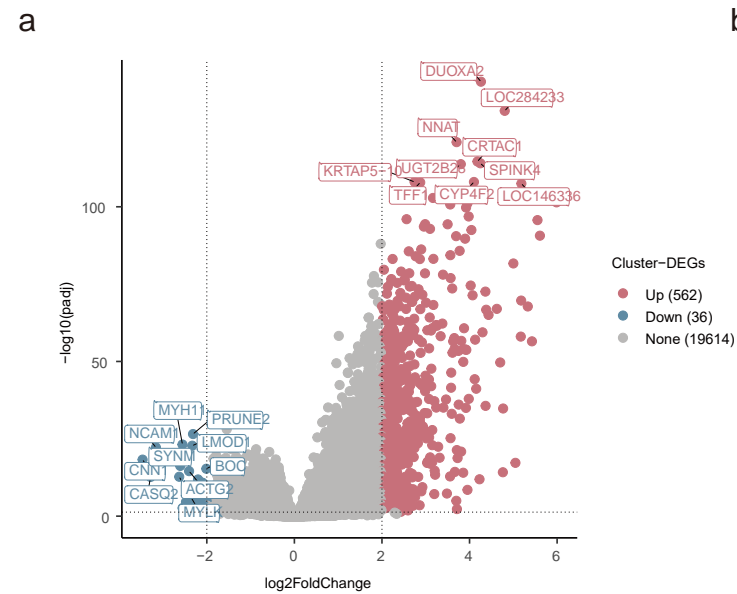
f





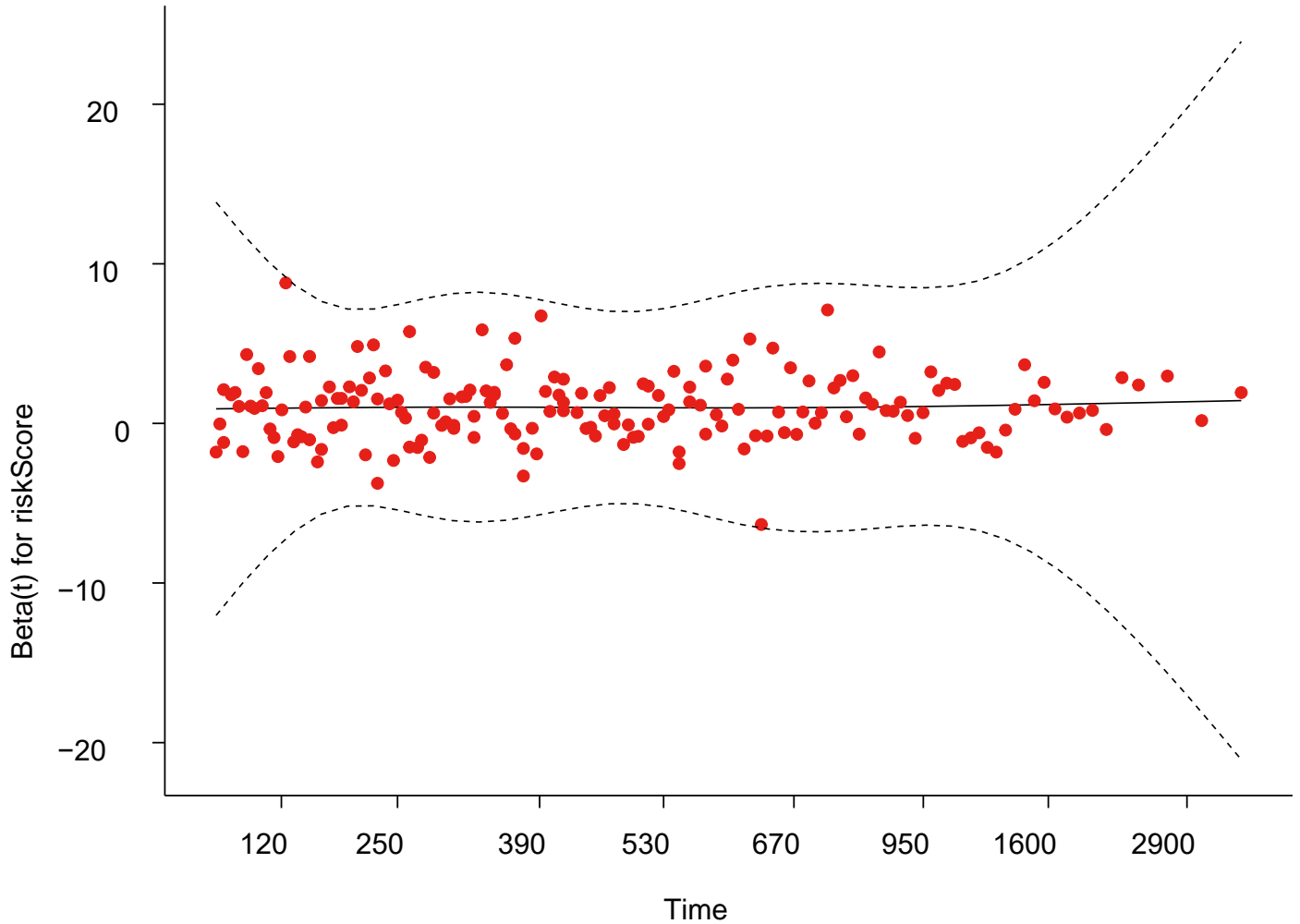
a**c****b****d**



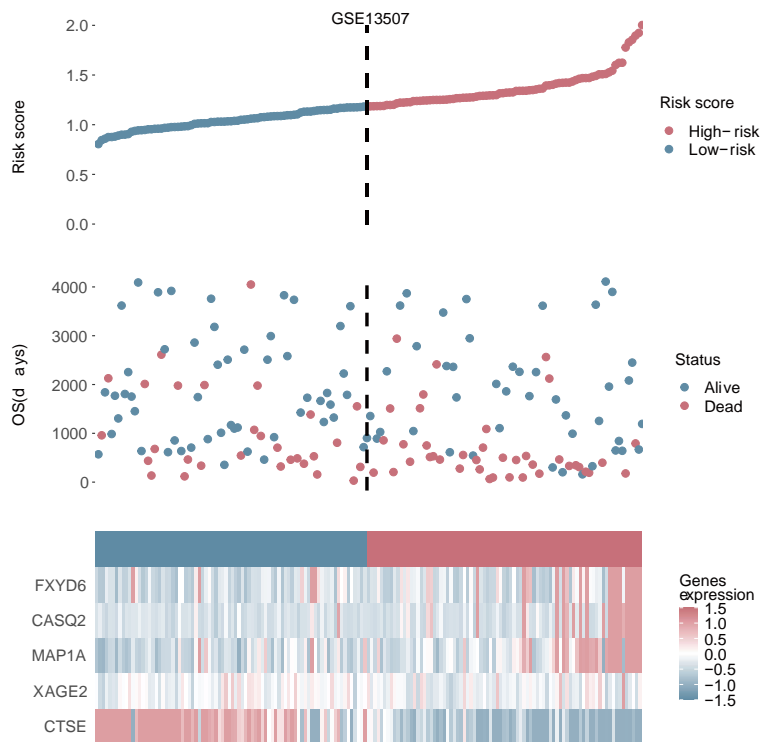


Global Schoenfeld Test p: 0.6699

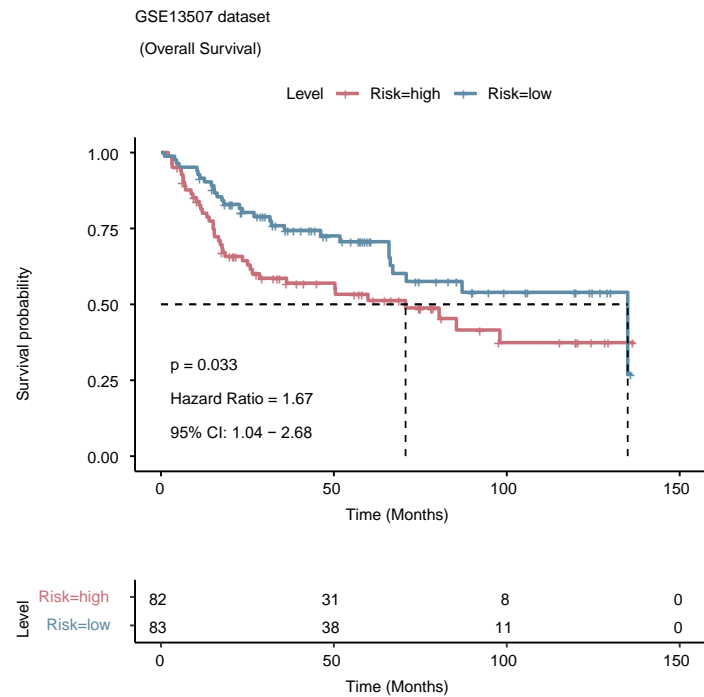
Schoenfeld Individual Test p: 0.6699



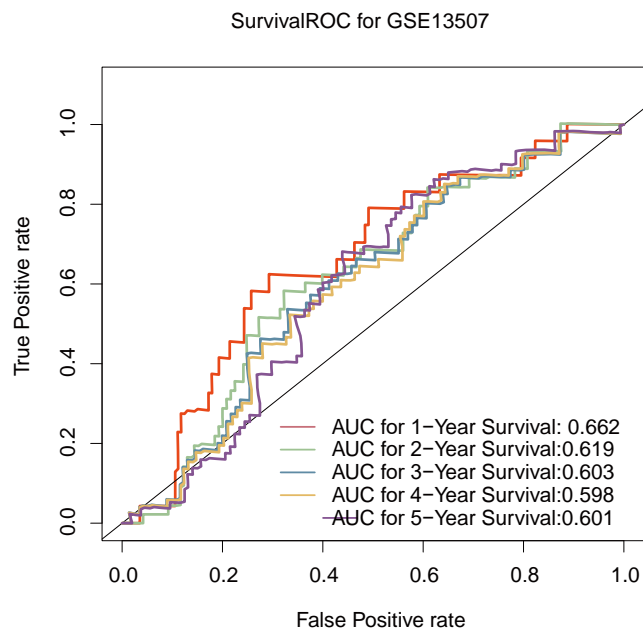
a

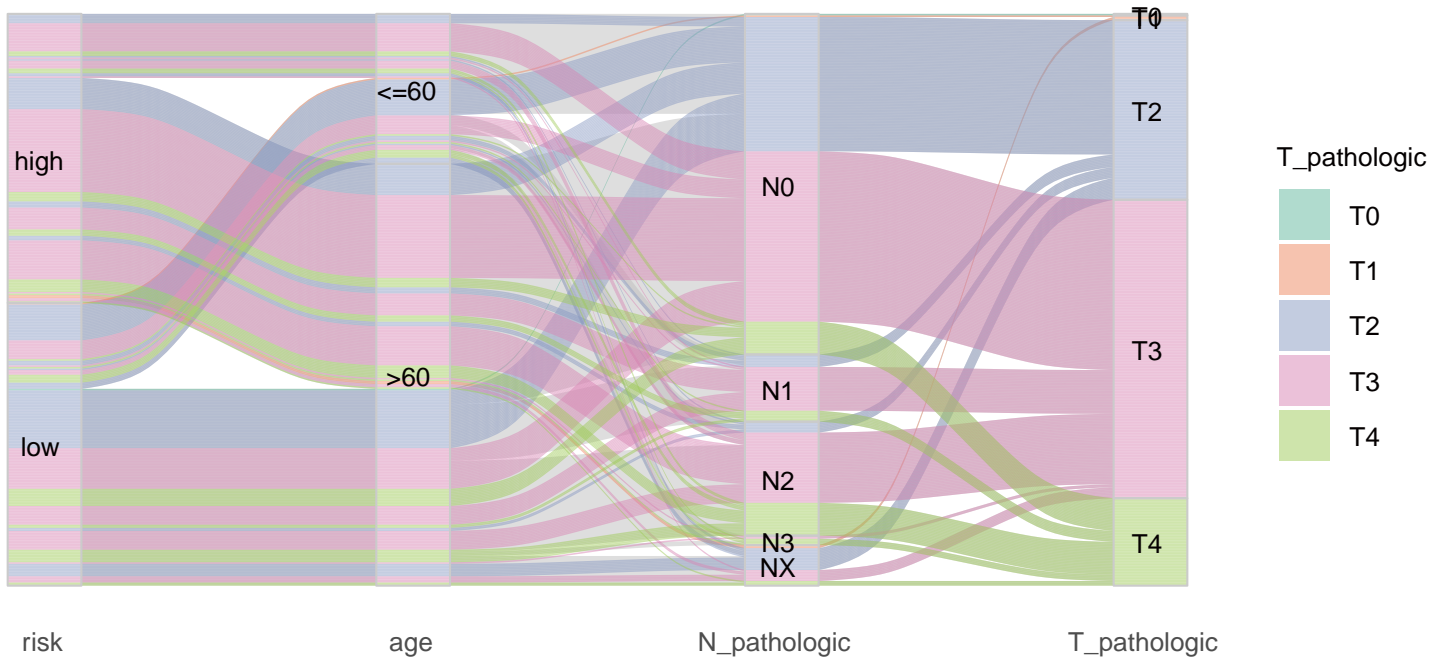


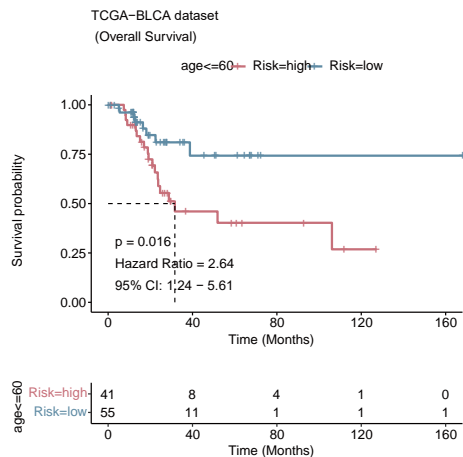
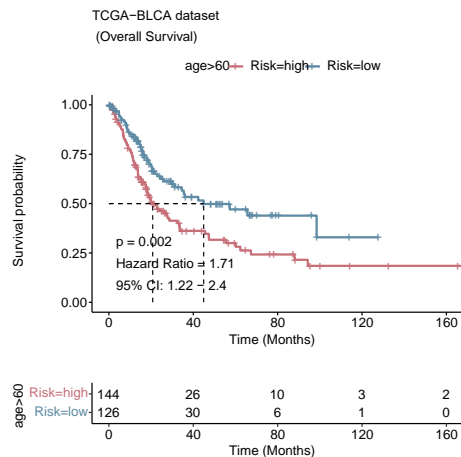
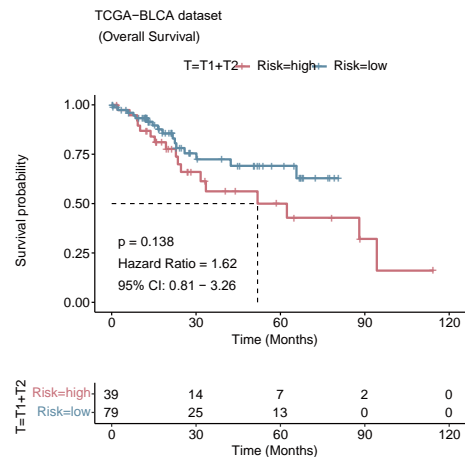
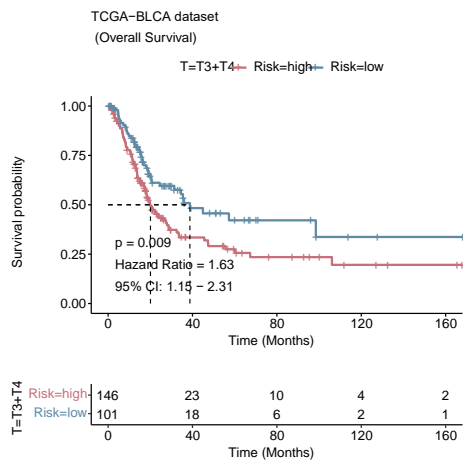
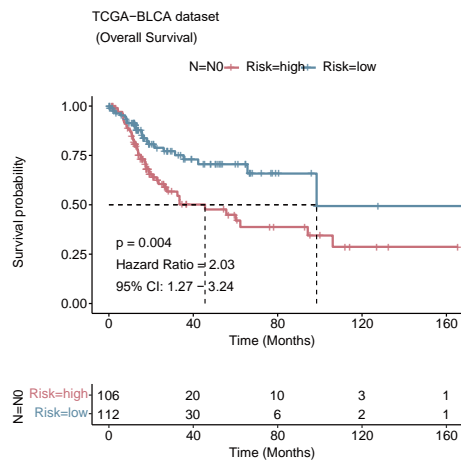
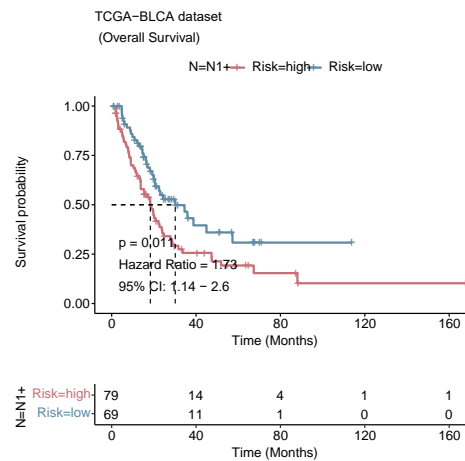
b



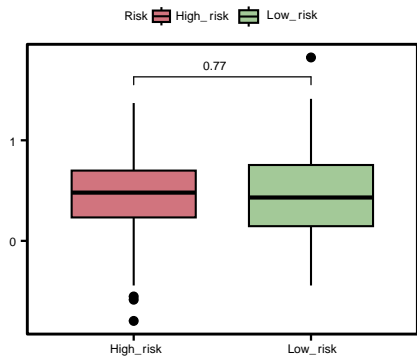
c



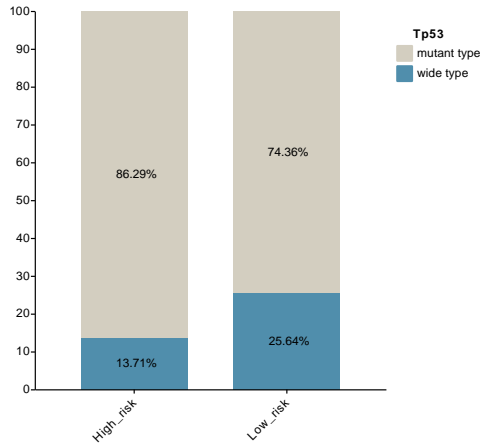


a**b****c****d****e****f**

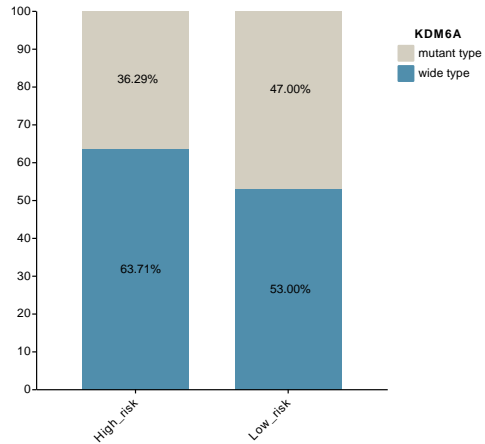
a



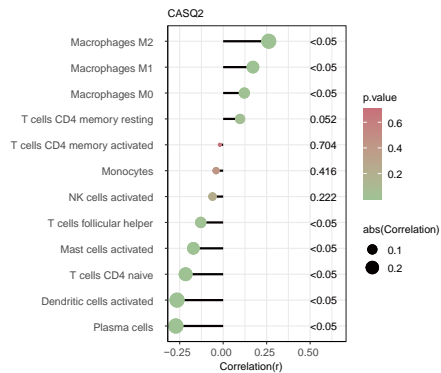
b



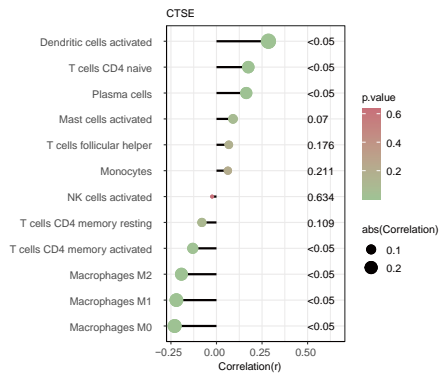
c



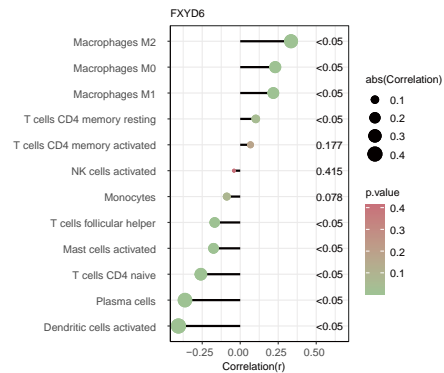
a



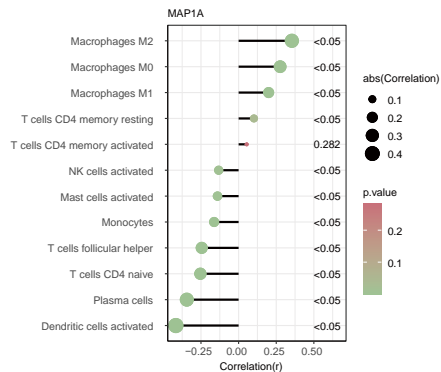
b



c



d



e

